76th International Astronautical Congress (IAC), Sydney, Australia, 29 September - 3 October 2025.


IAC-25.C1.IPB.9

# Mission design techniques for satellites operating in low-lunar orbits

**Mathilda Bolis [a,*], Elisa Maria Alessi[b], Camilla Colombo [a]**

[a] *Department of Aerospace Science and Technology, Politecnico di Milano, Via La Masa 34, 20156, Milan, Italy. mathilda.bolis@polimi.it, camilla.colombo@polimi.it*
[b] *Istituto di Matematica Applicata e Tecnologie Informatiche "Enrico Magenes", Consiglio Nazionale delle Ricerche, Via Alfonso Corti 12, Milano, 20133, Italy em.alessi@mi.imati.cnr.it*
[*]Corresponding author: mathilda.bolis@polimi.it

## Abstract

Several missions to the Moon are planned for the coming years. The international interest in the cislunar region is evident, as it is seen by many as the new frontier of space exploration and exploitation. However, designing a mission to reach an orbit close to the Moon is complex from many perspectives. Due to the non-linear dynamics characterising cislunar space, transfer design deals with chaotic trajectory behaviour, while the greater distance from Earth makes operations and the choice of satellite components complex. Moreover, miniaturised spacecraft are lately the favoured design choice for many missions, leading to a further increase in complexity due to limitations in the total $\Delta V$ budget.

In this paper, a set of techniques for transfer design and orbit selection for satellites operating in Low-Lunar Orbits (LLOs) is proposed. LLOs are interesting for many scientific applications, but from a mission analysis perspective, they have been less studied. The main objective of this work is to show how the minimisation of station-keeping and transfer costs can be addressed together, respecting, at the same time, the typical mission requirements of a CubeSat mission.

To minimise maintenance costs, a frozen orbit is proposed as the operational one. The frozen condition is designed with respect to the harmonics of the lunar gravitational field or the third body, depending on the altitude at which the LLO of interest is to be placed. On the other hand, an overview of the transfer design techniques by which such a LLO can be reached, minimising the $\Delta V$ budget, is presented, with a focus on the design of impulsive transfers. Strategies including low-energy transfers, weak stability boundary and endgame are considered, evaluated and compared in terms of total $\Delta V$ required, time of flight and sensitivity to the choice of the launch date.

The techniques described in this paper are applied to the design of LunPAN, a study funded by the European Space Agency within a new initiative on Small Missions for Exploration, and its inception, Destination the Moon. Its objective is to reach an LLO to measure the particle flux related to solar flares, albedo and galactic cosmic rays with the Pix.PAN and NeuPix instruments.

**Keywords: low lunar orbits, mission analysis, frozen orbits, Earth-Moon transfer design**

## Nomenclature

| | |
|---|---|
| $A/m$ $[m^2/s]$ | Area over mass ratio |
| $a$ [km] | Semimajor axis |
| $\beta[°]$ | Sun phase angle |
| $\Delta V$ [km/s] | Characteristic velocity increment |
| $e$ [-] | Eccentricity |
| $\Gamma$ [-] | First integral of motion |
| $i[°]$ | Inclination |
| $n$ [1/s] | Angular velocity |
| ndL [-] | Non-dimensional Length |
| ndT [-] | Non-dimensional Time |
| $\Omega[°]$ | Right Ascension of the Ascending Node (RAAN) |
| $\omega[°]$ | Argument of pericenter |
| $\Pi$ [-] | Second integral of motion |
| $r_a$ [km] | Apocenter radius |
| $r_p$ [km] | Pericenter radius |
| $r_{p_M}$ [km] | Perilune radius |
| $t$ [s] | Time |
| $T$ [s] | Orbital period |

## Acronym/Abbreviations

| | |
|---|---|
| BLT | Ballistic Lunar Transfer |
| CR3BP | Circular Restricted Three Body Problem |

| | |
|---|---|
| DRO | Distant Retrograde Orbit |
| ECI | Earth Centred Inertial |
| EM | Earth-Moon |
| ESA | European Space Agency |
| GCR | Galactic Cosmic Rays |
| GMAT | General Mission Analysis Tool |
| Id | Identification number |
| JC | Jacobi Constant |
| $L_1$ | First collinear Lagrange point |
| $L_2$ | Second collinear Lagrange point |
| LLO | Low Lunar Orbit |
| LME2000 | Lunar Mean Equator of date J2000 |
| LOI | Lunar Orbit Insertion |
| LunPAN | Lunar Particle ANalyser |
| MoonMJ2000Eq | Moon Mean Equator of J2000 |
| NRHO | Near Rectilinear Halo Orbit |
| SEP | Solar Energetic Particle |
| SEM | Sun-Earth-Moon |
| TBD | To Be Defined |
| TLI | Trans-Luna Injection |
| WSB | Weak Stability Boundary |

## 1. Introduction

The Moon has been a primary target for space exploration and scientific investigation since the beginning of the space age. With the Apollo program, lunar exploration reached its peak of public interest in the 20th century, culminating in the historic achievement of the first human landing. Afterwards, attention toward lunar missions did not rise again for several decades, only to increase significantly in recent years, supported by initiatives such as the Artemis program and the Lunar Gateway [1][2].

Today, the Moon is seen as a potential bridge between the Earth and the Solar System: it is close enough to Earth to allow for feasible crewed missions; yet, cislunar space presents dynamics governed by non-linear behaviours, which still pose significant scientific and engineering challenges. Numerous studies highlight the complexity of designing such missions, facing issues which are not typically considered for missions operating in the Earth neighbourhood.

Within this renewed framework of interest, many studies and projects, less ambitious than the large-scale human exploration programs cited above, have been proposed. Much about the Moon remains yet to be discovered; consequently, several recent missions have suggested the use of CubeSats or small satellites to investigate the lunar environment. This is also the case of the Lunar Particle ANalyser (LunPAN) mission, a study funded by the European Space Agency (ESA) within a new initiative on Small Missions for Exploration, and its inception, Destination the Moon. The primary objective of the LunPAN mission is to perform a comprehensive mapping of the particle spectra within the lunar radiation environment. The spacecraft is designed to deliver high-precision measurements of Galactic Cosmic Rays (GCRs), Solar Energetic Particles (SEPs), and lunar albedo particles, including charged particles, neutrons, and gamma rays, originating from the Moon's surface. By doing so, the mission is expected to advance the understanding of fundamental space physics and lunar geology, while also contributing to space weather forecasting and the assessment of radiation hazards for future explorations of the Moon.

Within the overall mission design, this paper focuses on the mission analysis, which represents a fundamental prerequisite for implementing the mission itself. From this perspective, it is essential to develop design strategies capable of identifying both an operational orbit and a corresponding transfer that are consistent with the mission objectives and requirements, while at the same time minimising the overall $\Delta V$ budget.

The operational orbit for LunPAN is selected as a Low Lunar Orbit (LLO). This choice, which will be justified and discussed in the following sections, is motivated by the fact that LLOs are particularly well suited to fulfilling the mission's scientific objectives. However, such a choice also introduces additional complexity compared to alternative solutions: LLOs are strongly perturbed by both the third-body effect, caused by the Earth in this case, and by the strongly irregular lunar gravitational field. As a consequence, without a careful selection of the orbital parameters, the spacecraft would be exposed to the risk of an uncontrolled impact on the lunar surface within a short timescale, unless a significant station-keeping effort is foreseen. Consequently, the design of the operational orbit focuses on searching for conditions under which LLOs exhibit a long-term bounded, "frozen" behaviour with respect to specific perturbations, depending on the chosen altitude. These dynamical features, supported by long-term simulations, provide a means to extend orbital stability while limiting the associated station-keeping requirements.

The choice of a LLO as the operational orbit complicates not only its definition, particularly in the attempt to limit station-keeping requirements, but also the design of a feasible low-cost transfer suitable for a small satellite. In the literature, numerous studies address Earth-to-Moon transfers; however, most of them focus primarily on reaching periodic orbits in cislunar space. These orbits are generally more stable than LLOs, and the transfer design can fully exploit three-body dynamics and associated invariant manifolds. This is not the case for LLOs: while similar dynamical techniques can still be employed, their application becomes significantly more challenging and comes at the price of a substantially higher $\Delta V$ budget.

This paper presents a set of techniques applicable to the design of a small satellite mission intended to operate in a LLO, with limited station-keeping efforts and $\Delta V$ budget, while simultaneously addressing both scientific and system requirements. In the following Sections, a trade-off analysis for the selection of the operational orbit is presented. Various options are then proposed for the orbit design, focusing on frozen or quasi-frozen conditions aimed at minimising or even eliminating the need for station-keeping. Subsequently, different transfer strategies to reach an LLO are evaluated and compared, some supported by numerical simulations and optimisation methods.

The objective of this work is to provide a framework for the pre-Phase A mission analysis of satellites intended to maintain a very low altitude around the Moon throughout their operational lifetime, highlighting the main challenges associated with this choice, as well as possible strategies to address them.

## 2. Mission objectives and spacecraft characteristics

The LunPAN mission aims to provide a comprehensive characterisation of the lunar radiation environment. Its primary payload, Pix.PAN [3], is a compact magnetic spectrometer based on thin silicon pixel sensors, optimised to measure penetrating charged particles in the 100 MeV–10 GeV range. A secondary, complementary payload, NeuPix, employs a similar innovative technology to detect albedo neutrons, gamma-rays, and lower-energy charged particles (10–100 MeV). Together, the instruments are capable of collecting important data on GCR, SEP and lunar albedo particles. The data retrieved would have great relevance to space physics, lunar geology, and radiation risk assessment for future exploration.

The nominal duration of the LunPAN mission is set at three years, as this timeframe will cover a significant part of the solar cycle and offers a high probability of detecting multiple strong solar particle events. The main scientific requirement of the mission is to maximise the retrieval of lunar albedo particles.

The dry mass of the mini-satellite is approximately 60 kg, and the spacecraft is equipped with an onboard chemical propulsion system.

## 3. Reference systems

Mission analysis for the LunPAN spacecraft is conducted using four different reference systems, each essential for addressing specific aspects of the satellite dynamics. The first is the Earth-Moon (EM) rotating reference frame, a rotating coordinate system. It is centred at the EM barycentre and:

- The $x$-axis is defined as the line going from the barycentre of the system to the Moon;
- The $z$-axis is perpendicular to the Moon's orbital plane;
- The $y$-axis completes the right-hand frame.

This reference frame is primarily used for designing the transfer trajectory and assessing frozen orbit conditions. Also, distances and times are considered dimensionless: a unit of length in the dimensionless frame, $ndL$, corresponds to 384399 km; a unit of time, $ndT$, is defined such that the angular velocity of the Earth and Moon rotating around their barycentre is equal to 1 in non-dimensional units.

When propagating given nominal orbits in a full dynamical model, the Moon Mean Equator of J2000 (MoonMJ2000Eq) reference system is used, a frame centred at the Moon and such that:

- The $x$-axis points along the line formed by the intersection of the Earth's mean equatorial plane and the mean ecliptic plane at the J2000 epoch;
- The $z$-axis is perpendicular to the Earth's mean equator at the J2000 epoch;
- The $y$-axis completes the right-hand frame.

The so-called Lunar Mean Equator of date J2000 (LME2000) has been used during the design phase, too. This reference frame is centred at the Moon and such that:

- The $x$-axis points toward the Moon's equinox of date J2000, where the Moon's equinox of date J2000 is defined as the intersection between the Moon's equator of date and the J2000 equator;
- The $z$-axis points toward the Moon's North Pole of date J2000;
- The $y$-axis completes the right-hand frame.

Finally, for the transfer design, the Earth Centred Inertial (ECI) reference frame has been employed too. This inertial system is centred at the Earth's centre of mass and defined as follows:

- The $x$-axis is directed toward the mean equinox of J2000.
- The $z$-axis is aligned with the Earth's mean rotation axis at J2000.
- The $y$-axis completes the right-hand frame.

## 4. Operational orbit trade-off

An initial trade-off is conducted to support the selection of the most suitable type of operational orbit. The key requirements for choosing it are for the spacecraft to operate in the cislunar domain, close to the Moon, and for it to be placed on an operational orbit allowing for the 5% particle retrieval Poisson level to be reached within one month.

Various families of orbits can be defined within cislunar space, including Low Lunar Orbits (LLOs), Halo and Near-Rectilinear Halo Orbits (NRHOs) at both the Lagrangian collinear points $L_1$ and $L_2$, Distant Retrograde Orbits (DROs), and others. Given the requirement that the mean distance between the orbit and the Moon must remain low throughout the entire operational lifetime (i.e., three years), while also keeping the overall mission $\Delta V$ budget within strict limits, four families of candidate orbits have been selected for a trade-off analysis, to determine which orbit type best satisfies the particle retrieval requirement:

- **LLOs**. Both circular and elliptical LLOs are considered. LLOs remain in close proximity to the Moon throughout their entire orbital period, which makes them an attractive option as operational orbits for missions requiring continuous observation of the lunar surface. However, such orbits are strongly influenced both by the gravitational perturbations of the third body, in this case, the Earth, and by the non-uniformities of the lunar gravitational field. As a consequence, LLOs are subject to highly non-linear dynamics, and long-term dynamical modelling is necessary to obtain a reliable understanding of their evolution over the mission duration. This applies to both circular and elliptical LLOs, although, as will be discussed later, specific techniques can be employed to carefully select the orbital elements to mitigate the perturbative effects of the Earth and the Moon on the orbit. Nevertheless, due to these dynamical characteristics, LLOs typically require a relatively high station-keeping budget, as well as significant $\Delta V$ for any autonomous transfer manoeuvres.

- **Circular LLOs.** For the circular LLO option, ten candidates are considered in the trade-off analysis. As a first approximation, these orbits are defined by progressively increasing the altitude above the lunar surface in $50$ km increments, starting from an initial altitude corresponding to the Moon's radius, equal to $1737.4$ km, plus $50$ km. At this stage, the orientation of the orbits in space is not defined, since it is not of interest for this preliminary trade-off analysis. Data relative to the first approximation of the orbits considered are reported in Table 1, and, in Figure 1, a graphical representation of the same test cases is shown.

Table 1. Circular LLOs - Test cases considered.

| Id [-] | $a$ [km] | $T$[s] |
|---|---|---|
| 1 | 1787.4 | 6780.9 |
| 2 | 1837.4 | 7067.5 |
| 3 | 1887.4 | 7357.9 |
| 4 | 1937.4 | 7652.2 |
| 5 | 1987.4 | 7950.3 |
| 6 | 2037.4 | 8252.2 |
| 7 | 2087.4 | 8557.9 |
| 8 | 2137.4 | 8867.2 |
| 9 | 2237.4 | 9496.7 |
| 10 | 2737.4 | 12851.8 |

- **Elliptical LLOs.** For the elliptical LLOs option, the orbits' eccentricity is chosen to have a pericenter altitude equal to 20 km, given the same semimajor axis of the circular orbits. Data relative to the eight candidates chosen to represent elliptical LLOs in the trade-off analysis are reported in Table 2, and shown in Figure 2.

- **NRHOs**. Both NRHOs in EM-$L_1$ and EM-$L_2$ are considered. NRHOs are periodic solutions of the

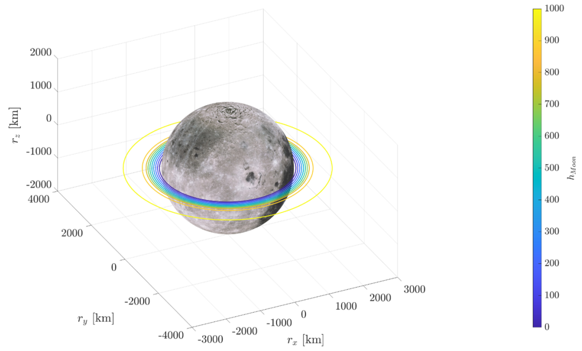


Fig. 1. Circular LLOs - Graphical representation of test cases considered. The value on the colour bar represents the altitude from the Moon. The orientation of the orbits is generic at this stage of the analysis.

Table 2. Elliptical LLOs - Test cases considered.

| Id [-] | $a$ [km] | $e$ [-] |
|---|---|---|
| 1 | 1787.4 | 0.016 |
| 2 | 1837.4 | 0.043 |
| 3 | 1887.4 | 0.068 |
| 4 | 1937.4 | 0.092 |
| 5 | 1987.4 | 0.115 |
| 6 | 2037.4 | 0.137 |
| 7 | 2237.4 | 0.214 |
| 8 | 2737.4 | 0.358 |
| $r_a$ [km] | $r_p$ [km] | $T$ [s] |
| 1815.9 | 1758.8 | 6780.9 |
| 1916.4 | 1758.4 | 7067.5 |
| 2015.7 | 1759.1 | 7357.9 |
| 2115.6 | 1759.2 | 7652.2 |
| 2215.9 | 1758.8 | 7950.3 |
| 2316.5 | 1758.3 | 8252.2 |
| 2716.2 | 1758.6 | 8557.9 |
| 3717.4 | 1757.4 | 8867.2 |

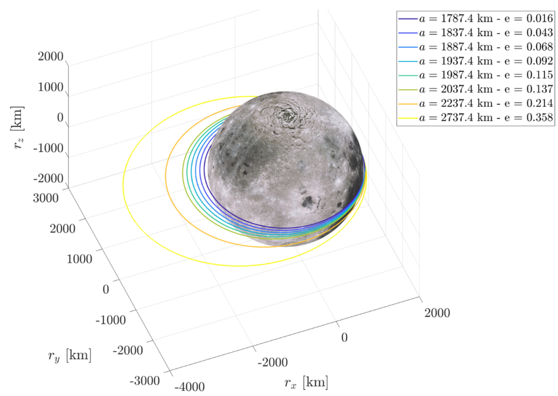


Fig. 2. Elliptical LLOs - Graphical representation of test cases considered. The values of a and e represent semimajor axis and the eccentricity of the orbits considered. The orientation of the orbits is generic at this stage of the analysis.

Circular Restricted Three-Body Problem (CR3BP) and represent a specific subset of the broader Halo orbit families associated with both the $L_1$ and $L_2$ libration points. Like LLOs, they can be of considerable interest for lunar observation missions, as they provide regions of close approach with the lunar surface thanks to their low perilunes. At the same time, compared to LLOs, NRHOs are characterised by much higher apolunes, making the overall orbits' mean distance from the Moon higher than in the previous case. The main advantage of these orbital family lies in their stability within the EM CR3BP. While some $\Delta V$ is still required for station-keeping, primarily to counteract perturbations from additional gravitational bodies and the irregularities of the lunar gravity field, the required budget is generally lower than that required for maintaining spacecraft on LLOs. Furthermore, NRHOs present greater flexibility in terms of transfer design, offering a variety of feasible transfer options with relatively modest $\Delta V$ requirements, even when a dedicated launch is not available.

- **EM-$L_1$ NRHOs** Characteristics such as the Jacobi Constant (JC) and the perilune radius are reported in Table 3 for the orbits considered in the analysis, shown in Figure 3

Table 3. NRHOs in $L_1$ - Test cases considered.

| Id [-] | JC [-] | $r_{p_M}$ [km] |
|---|---|---|
| 1 | 2.9922 | 1800.3 |
| 2 | 2.9938 | 1865.04 |
| 3 | 2.9953 | 1935.49 |
| 4 | 2.9969 | 2007.57 |
| 5 | 2.9984 | 2093.83 |
| 6 | 3.0001 | 2188.67 |
| 7 | 3.0015 | 2275.97 |
| 8 | 3.0029 | 2373.22 |

- **EM-$L_2$ NRHOs** Data relative to the orbits considered in the analysis are reported in Table 4, and shown in Figure 4

Table 4. NRHOs in $L_2$ - Test cases considered.

| Id [-] | JC [-] | $r_{p_M}$ [km] |
|---|---|---|
| 1 | 3.0704 | 1793.91 |
| 2 | 3.0695 | 1879.32 |
| 3 | 3.0686 | 1966.41 |
| 4 | 3.0676 | 2067.96 |
| 5 | 3.0667 | 2158.59 |
| 6 | 3.0659 | 2250.86 |
| 7 | 3.0651 | 2344.75 |
| 8 | 3.0642 | 2454.03 |

A trade-off analysis has been performed for all the previously introduced orbits to determine which of them

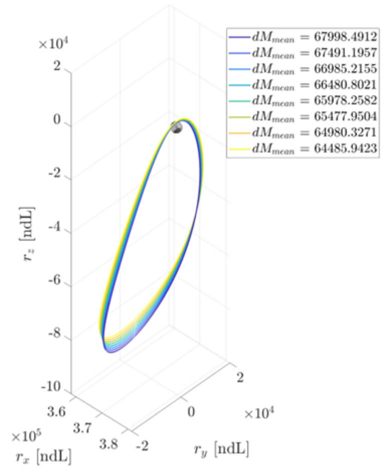


Fig. 3. NRHOs in $L_1$ - Graphical representation of test cases considered. The colour represents the mean distance between the orbits and the Moon surface.

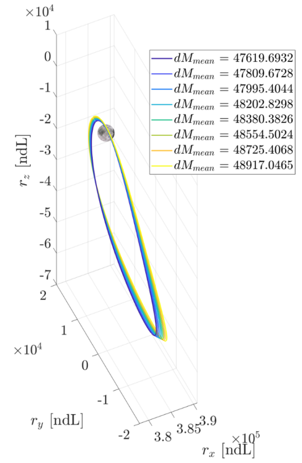


Fig. 4. NRHOs in $L_2$ - Graphical representation of test cases considered. The colour represents the mean distance between the orbits and the Moon surface.

satisfies the requirement of achieving a 5% particle retrieval Poisson level within one month. For each orbit, the time required to reach the specified particle flux Poisson level measurable by the payloads on board LunPAN is approximated as a function of the mean distance from the Moon. At this stage of the analysis, the orientation of the candidate orbits is not relevant, since the particle flux is assumed to be isotropic. In addition to particles originating from solar flares, which require only the spacecraft to be within the path of the flare when it occurs, the payloads will also measure albedo and GCR particles. Near the Moon, the GCR flux is significantly modulated by the shadowing effect of the Moon, which increases as the spacecraft approaches the lunar surface. Conversely, the flux of lunar albedo particles increases with decreasing altitude. The results of this analysis, for all the particles of interest, are presented in Figures 5 to 10, providing a clear comparison of the time needed to reach the required Poisson level across different orbits.

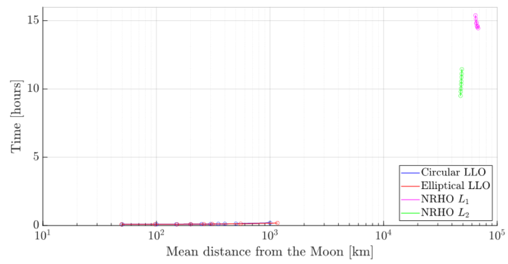


Fig. 5. Time needed to reach the required electron positron albedo statistics level as a function of mean distance from the Moon for 4 types of orbit, circular LLOs, elliptical LLOs, NRHOs around $L_1$ and NRHOs around $L_2$.

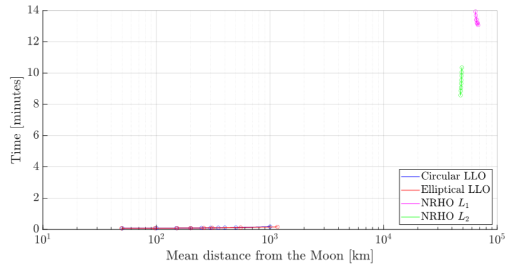


Fig. 6. Time needed to reach the required gamma photons albedo statistics level as a function of mean distance from the Moon for 4 types of orbit, circular LLOs, elliptical LLOs, NRHOs around $L_1$ and NRHOs around $L_2$.

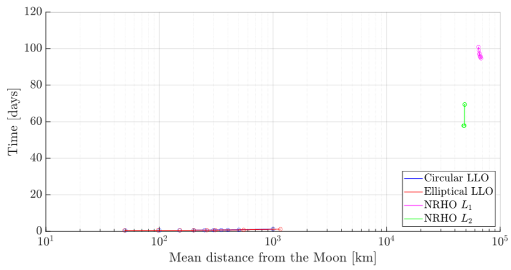


Fig. 7. Time needed to reach the required neutron fast statistics level as a function of mean distance from the Moon for 4 types of orbit, circular LLOs, elliptical LLOs, NRHOs around $L_1$ and NRHOs around $L_2$.

As expected, the lunar albedo particle flux reaches the 5% Poisson level faster when the spacecraft is closer to the Moon, whereas the GCR flux increases with distance. However, as shown in Figure 10, the GCR flux remains significantly higher than the lunar albedo one. Consequently, the orbit selection focuses on minimising the time required to reach the 5% measurement level for albedo particles. The analysis indicates that LLOs are the most favourable choice from a mission objective

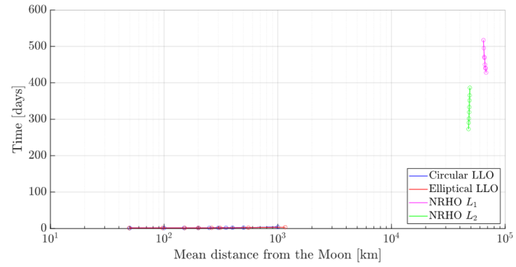


Fig. 8. Time needed to reach the required neutron slow statistics level as a function of mean distance from the Moon for 4 types of orbit, circular LLOs, elliptical LLOs, NRHOs around $L_1$ and NRHOs around $L_2$.

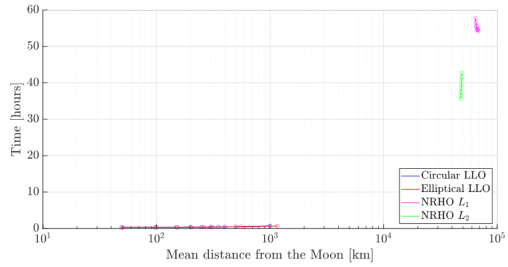


Fig. 9. Time needed to reach the required protons albedo statistics level as a function of mean distance from the Moon for 4 types of orbit, circular LLOs, elliptical LLOs, NRHOs around $L_1$ and NRHOs around $L_2$.

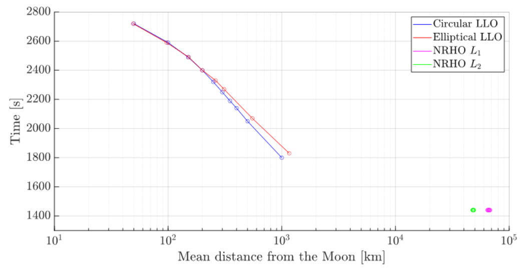


Fig. 10. Time needed to reach the required protons GCR statistics level as a function of mean distance from the Moon for 4 types of orbit, circular LLOs, elliptical LLOs, NRHOs around $L_1$ and NRHOs around $L_2$.

perspective. For slow neutrons, which have the lowest particle flux among the considered particles, the 5% level can be achieved within one to four days, depending on the altitude of the selected LLO.

The conclusions drawn from this analysis are that LLOs provide greater scientific return, with no significant differences identified between circular and elliptical orbits. As Figures 5 to 10 show, if LLOs are considered, the 5% Poisson error level can be reached within minutes (GCR) to days (neutrons). NRHOs offer more advantages in terms of transfer and station-keeping costs. However, when NRHOs are considered, the 5% Poisson level can only be reached after minutes (GCR) to years (neutrons). Therefore, for lunar albedo particles, and so for science objectives which depend on their measurement, it is necessary to select an LLO orbit as operational. Comparatively, GCR particles have a much higher flux and are primarily affected by the shadow cast by the Moon itself. Therefore, the differences between NRHO and LLO orbits are not significant.

To select an NRHO as the operational orbit is still possible and will be considered in the final trade-off for completeness, but would imply changing the payloads' architecture to better comply with mission objectives.

## 5. Operational orbit design

The requirements posed by the main payload lead to the selection of LLOs as the preferred option among those considered in the operational orbit trade-off. However, as also stated earlier, LLOs present certain disadvantages compared to alternative solutions: they are subject to significant perturbations, primarily from the Earth third-body influence and the non-uniformity of the lunar gravitational field; a satellite orbiting on them can experience longer eclipse periods than one orbiting on other types of orbits (e.g., NRHOs); and a transfer to an LLO may require a higher $\Delta V$ than transfers to other orbits. Moreover, the final selection of the operational orbit is expected to be strongly influenced by the choice of launcher, which has not yet been defined.
Two options are considered for the selection and design of the operational orbit. In OPTION 1, a dedicated launch is assumed, and operational orbit characteristics are not constrained by the launcher, providing full flexibility in defining orbital parameters. In a second scenario, OPTION 2, a rideshare launch is considered: the orbital parameters of the LLO in which the launcher injects the spacecraft at the Moon are imposed by launcher constraints. In this second option, some considerations about how mission planning would be affected are to be considered, particularly in terms of station-keeping requirements. As for OPTION 1, the following considerations apply:

- An operational orbit which shows a frozen behaviour would be highly preferred, as it corresponds to specific orbital conditions where the long-term variations in orbital parameters due to perturbations are bounded. Selecting such an orbit as the operational one would reduce station-keeping costs compared to other alternatives. This assumption will be verified through numerical simulations, but it is generally considered valid.
- For all LLOs previously analysed, the science requirements on payload measurements are met. On the other hand, orbits closer to the Moon will theoretically be more expensive to reach if direct insertion at the Moon by the launcher is not available, and more expensive to maintain due to the lunar gravitational potential. Furthermore, these same orbits will be subject to longer eclipse times, as will be discussed later. For these reasons, an orbit with a greater mean distance from the Moon would be preferred.

In view of the above, for OPTION 1, an LLO at 1000 km of altitude is considered. The possibility of choosing the inclination in such a way that the orbit will be frozen with respect to the dominant perturbations is investigated. According to [4], below an altitude of 500 km, it is convenient to design a frozen condition with respect to the perturbation due to the lunar gravitational harmonics, above 500 km with respect to the third-body one, in this case mainly due to the Earth. The latter approach is followed.

Regarding OPTION 2, the initial orbital parameters of the LLO into which the spacecraft is injected by the launcher are predetermined. Preliminary analyses are carried out to evaluate the evolution of these orbits. At this stage, two alternatives are being considered: the first is to adopt the injected orbit as the operational one (i.e., having an a priori defined operational orbit); the second option is to perform a manoeuvre close to the Moon to transfer the spacecraft from the initial LLO to a more favourable frozen or quasi-frozen condition. This aims to reduce maintenance costs, but an eventual shape or plane change manoeuvre would incur additional expenses.
Even assuming it is feasible and requires a relatively modest $\Delta V$ to place the spacecraft into a quasi-frozen condition, the associated station-keeping costs may be higher than those foreseen in OPTION 1, mainly because of a fixed lower altitude.

### *5.1 OPTION 1*

#### 5.1.1 First approximation

Assuming a high altitude LLO, the third-body perturbation due to the Earth is the first effect to analyse to model a frozen orbit. Considering it as the only perturbation in the system, the orbital eccentricity varies in the long term, while the semi-major axis remains constant. The eccentricity $e$ variation is coupled with the variation in inclination $i$ and argument of pericenter $\omega$, and it is possible to compute libration regions where the variation in $(e, \omega)$ is bounded in a given range.

To this end, we adopt the formulation shown in [5, 6, 7, 4, 8], that doubly-averages the first-order perturbation of the third-body taking as reference plane the lunar orbital plane. By computing the equilibrium points for a well-defined value of the first integral of the system, it is possible to identify the regions of interest, as shown in Fig. 11. The behaviour changes from libration to circulation at well-defined values of inclination.

The problem will not be analysed in detail in this context; however, it is important to note that quasi-circular orbits could be a suitable choice for operational purposes, and that the natural increase in eccentricity for

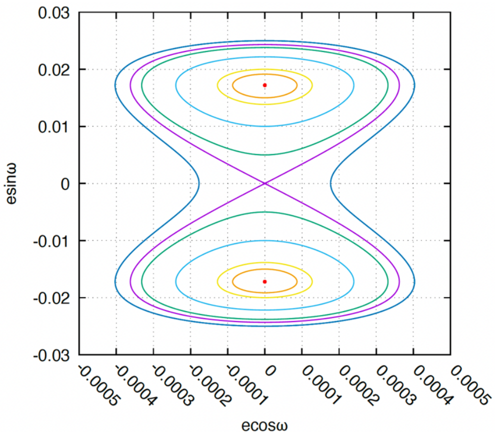


Fig. 11. Level curves associated with Π for the phase space corresponding to the equilibrium point at $e = 0.0172$.

an orbit with $a = 2737.4$ km should preferably remain below $0.358$ (see Table 2). If a frozen condition corresponding to an inclination close to $39.23°$ and an eccentricity near zero in the lunar orbital plane are considered, this would be ensured in the simplified approximation. The next step is to evaluate the effects of lunar gravitational harmonics on this type of orbits to verify whether these frozen conditions remain sufficiently stable in the long term and are not significantly perturbed by the Moon's gravitational field.

#### 5.1.2 Full model simulation

From the considerations above, the orbital parameters of the operational orbit for OPTION 1 correspond to those listed in Table 5, defined with respect to a coordinate system whose reference plane is the lunar orbital plane. This reference system corresponds to the EM rotating reference frame (see Section 3).

Table 5. Orbital parameters of the operational orbit - OPTION 1.

| $a$ [km] | $e$ [-] | $i$ [°] | $\Omega$ [°] | $\omega$ [°] |
|---|---|---|---|---|
| 2738 | 0.001 | 40 | 0 | 90 |

The selected orbit is propagated for 366 days, by means of the General Mission Analysis Tool (GMAT) software tool [9], considering the perturbations due to Sun, Earth, Venus, Mars, Jupiter, the lunar gravitational potential up to degree and order 50 (LP165P model [10]), and the solar radiation pressure ($A/m = 0.001\ m^2/kg$), in the MoonMJ2000Eq reference system.
Two propagations are performed, assuming two different initial epochs, 22 Sept 2029 at $11.29 : 00$h, and 1 Feb 2030 at $19 : 00 : 00$h. In Figure 12 and Figure 13, the variation of the altitude at the Moon, of the eccentricity, inclination and argument of pericenter in the MoonMJ2000Eq reference system is shown. The altitude is well preserved, while there is a significant drift in orbital inclination, which should be better evaluated in the LME2000 reference system, too.

#### 5.1.3 Eclipse analysis

The eclipse analysis is performed by modelling the relative motion between the Earth and the Moon as in the EM rotating reference frame, with the Sun rotating around the centre of the reference frame with a constant angular velocity. The Sun is assumed in a circular orbit of radius 1 AU around the EM barycentre, with an inclination of $5°$ with respect to the EM plane [11]. The position of the Sun is computed as a function of a phase angle $\beta$, which represents the evolution of the position of the Sun in the system during a year (365 days). The model considered is represented in Figure 14.

The basic eclipse geometry considered is modelled as represented in Figure 15 [12]. Eclipses occur within the umbra and penumbra regions.

The umbra region is totally eclipsed by the primary body considered, which in this case is either the Earth or the Moon; while the penumbra region is only partially obscured by the primary. Thanks to a series of geometric relations, it is possible to compute the percentage of orbital period for which a given orbit undergoes an eclipse condition, as the position of the Sun in the system varies. As the orbit is operative around the Moon, it is subject to both the Moon's and the Earth's shadow. It was noticed that the eclipse duration changes due to the inclination and the altitude of the orbit over the surface of the Moon: as the altitude increases, the eclipse duration decreases, and the same is true for the inclination. If necessary, the altitude and inclination could be increased to decrease the eclipse time on the operational orbit.
For the orbit defined in Table 5, of which the period is equal to 3 h and 34.27 min, the results shown in Figure 16 and Figure 17 are obtained.

This results in one day of eclipse caused by the Earth and 42 days and 1.2 hours of eclipse caused by the Moon on the orbit considered over one year.

### *5.2 OPTION 2*

#### 5.2.1 Full model simulation

In this scenario, LunPAN will take advantage of a rideshare launch opportunity. As previously mentioned, in this case, the operational orbit cannot be freely selected from scratch, but must remain close to the one on which the launcher will release the spacecraft. The injection orbit will depend on the requirements of the primary mission financing the launch, and therefore cannot be independently optimised for LunPAN. At present, many of the parameters defining these orbits are still to be defined. Nevertheless, as a starting point, a full-model simulation has been carried out for a subset of candidate orbits proposed by the launcher company, namely:

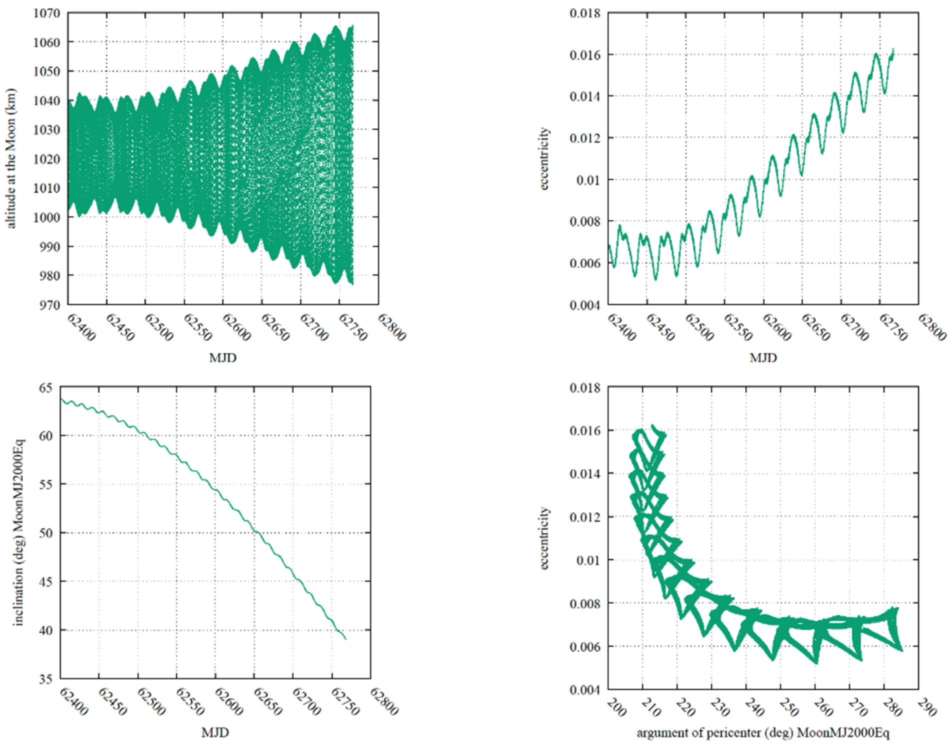


Fig. 12. Evolution of elements of interest for the operational orbit selected – OPTION 1. Initial epoch: 22 Sept 2029 at 11.29 : 00 h.

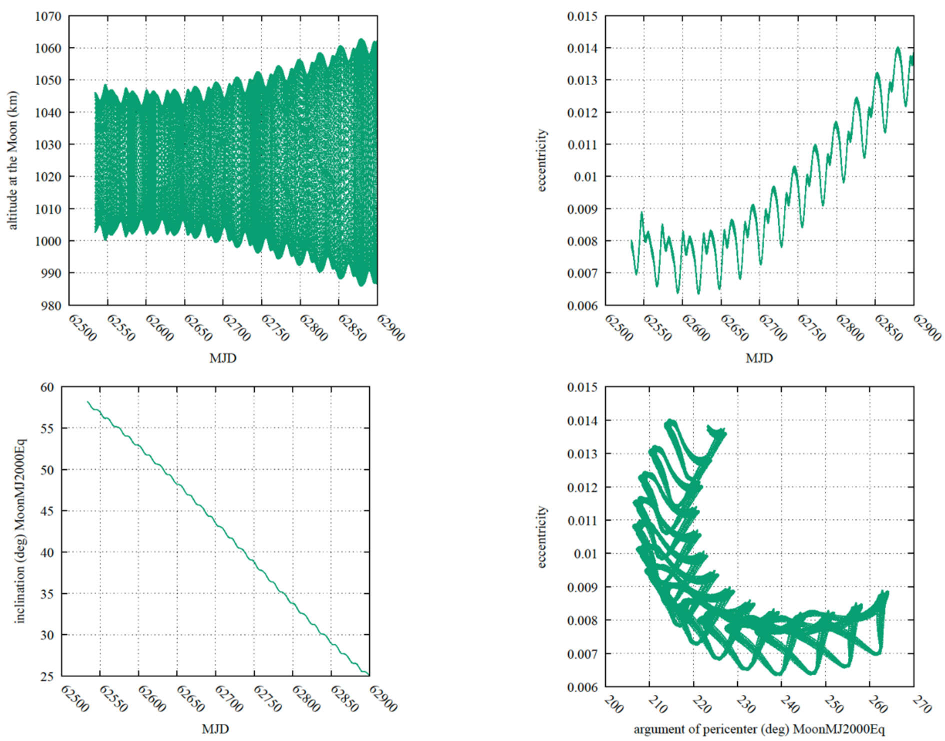


Fig. 13. Evolution of elements of interest for the operational orbit selected – OPTION 1. Initial epoch: 1 Feb 2030 at 19 : 00 : 00 h.

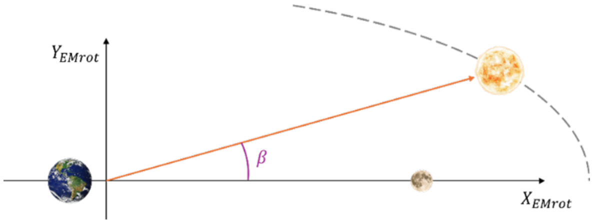


Fig. 14. Schematic model considered for the motion of the Sun around the EM barycentre.

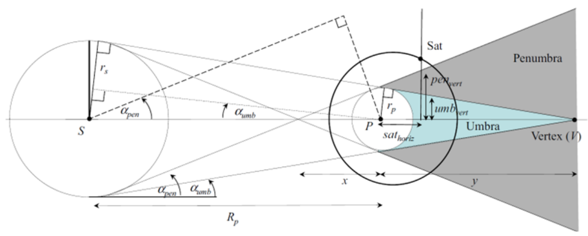


Fig. 15. Eclipse model, schematic representation [12].

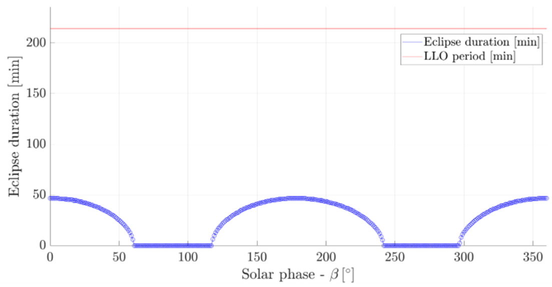


Fig. 16. Duration of the eclipse phase caused by the Moon over one period of the operational orbit as a function of the phase angle of the Sun – OPTION 1.

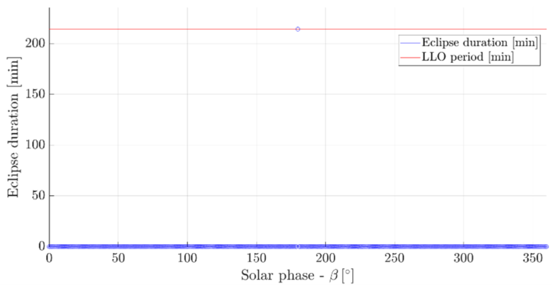


Fig. 17. Duration of the eclipse phase caused by the Earth over one period of the operational orbit as a function of the phase angle of the Sun – OPTION 1.

- **CASE 1:** 100 km x 4100 km orbit, $a = 3837.4$ km, $e = 0.5212$
- **CASE 2:** 100 km circular orbit, $a = 1837.4$ km, $e = 0$
- **CASE 3:** 100 km x 800 km orbit, $a = 2187.4$ km, $e = 0.16$

The orientation of the orbits in CASE 1 and CASE 2 is not yet fixed. In contrast, the orientation for CASE 3 is predefined. This latter case is only briefly introduced in this section and will be discussed in greater detail later.

A few tests were run to see the long-term behaviour of CASE 1, a 100 km x 4100 km orbit. The evolution of the spacecraft altitude for three different values of inclination equal to 70°, 20° and 56° in the MoonMJ2000Eq reference system, is shown in Figure 18. Also, in the third case, $\Omega$ is fixed equal to 90° instead of 0°.

For CASE 2, with a 100 km altitude circular orbit, the work in [13] shows that an impact with the lunar surface would take place in about 150 days. In [14], it is shown how this estimate depends on the values of inclination and right ascension of the ascending node, which, in this case, are still TBD by the primary mission.

If this option is selected, it is possible to consider designing a frozen condition with respect to the lunar gravitational harmonics, as suggested in [15]. For instance, for a semi-major axis of 1861 km, the author suggested stable orbits like the ones that can be found in Table 6, where orbital parameters are expressed with respect to the coordinate system taking as reference plane the EM orbital plane.

Table 6. Frozen orbit conditions with respect to the Moon gravitational harmonics. The reference plane is the lunar orbital plane.

| **e [-]** | $\boldsymbol{i}$ **[°]** | $\boldsymbol{\omega}$ **[°]** |
|---|---|---|
| 0.0388 | 10 | 90 |
| 0.0537 | 45 | 270 |
| 0.0530 | 54 | 90 |
| 0.0177 | 80 | 90 |

A full model simulation was run for one year, considering the fourth initial condition listed below, starting from February 2, 2030, at $19:00$. The output seems very favourable, as shown in Figure 19. More simulations considering different initial epochs should be run to consolidate this result.

### 5.2.2 Eclipse analysis

The eclipse analysis defined in Section 5.1.3 is repeated also for an orbit having the Keplerian parameters in the EM rotating frame reported in Table 7.

Table 7. Orbital parameters of the selected case.

| $\boldsymbol{a}$ **[km]** | $\boldsymbol{e}$ **[-]** | $\boldsymbol{i}$ **[°]** | $\boldsymbol{\Omega}$ **[°]** | $\boldsymbol{\omega}$ **[°]** |
|---|---|---|---|---|
| 1861 | 0.0177 | 80 | 0 | 90 |

The total eclipse time caused by the Earth is equal to one day; the one caused by the Moon lasts 90 days and 37.08 minutes.

## 6. Transfer trajectory design

Designing a transfer trajectory from Earth to the Moon presents significant challenges, primarily due to the com-

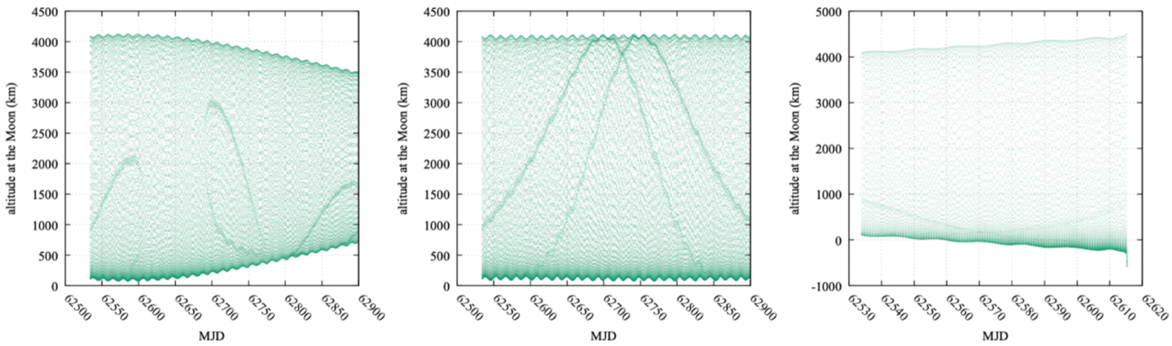


Fig. 18. Evolution of the satellite altitude with respect to the Moon for three different values of inclination. From left to right: $i = 70°$, $\Omega = 0°$; $i = 20°$, $\Omega = 0°$; $i = 56°$, $\Omega = 90°$ – OPTION 2.

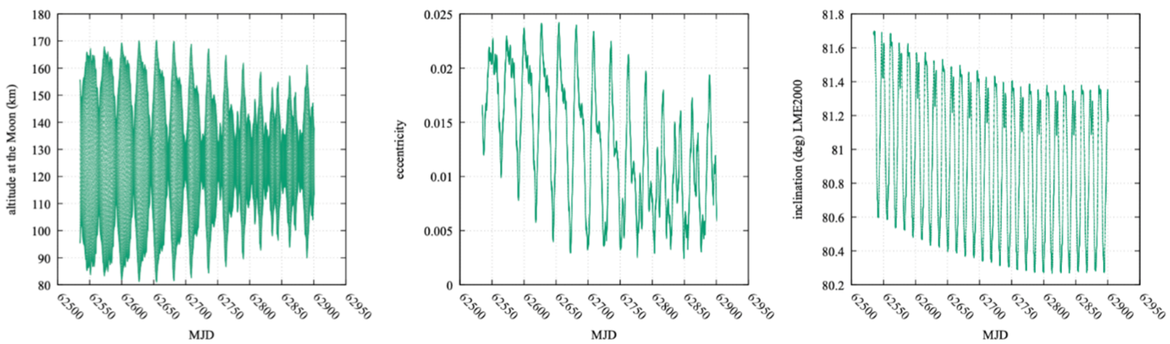


Fig. 19. Evolution of elements of interest for the operational orbit selected – Frozen condition with respect to the Moon gravitational harmonics.

plex and highly sensitive dynamical environment that characterises cislunar space. Even small variations in the initial conditions can lead to vastly different trajectories, each associated with substantially different $\Delta V$ requirements. This sensitivity is a consequence of the gravitational relationship between the Earth, Moon, and Sun, which gives rise to non-linear dynamics and necessitates high-precision modelling to achieve reliable and predictable results.

The primary requirement for the transfer trajectory design is that, if a direct injection into the operational lunar orbit is not feasible, the launcher must at least provide the Trans-Lunar Injection (TLI) impulse necessary to place the spacecraft onto its transfer trajectory. Note that TLI refers to a condition in which the first impulse is given to insert the spacecraft on a transfer trajectory to the Moon/on a trajectory close to the Moon.

Several transfer strategies respecting this constraint have been proposed and studied in the literature to address EM transfer design. These include, among others, Weak Stability Boundary (WSB) transfers, or Ballistic Lunar Transfers (BLTs); endgame transfers; and low-energy transfers, each offering distinct advantages in terms of $\Delta V$ [16][17][18]. The main characteristics and trade-offs for these transfer design options are summarised in Table 8. Note that Lunar Orbit Insertion (LOI) refers to the condition in which the impulse is given to insert the spacecraft from the transfer trajectory into the operational LLO.

Each transfer option presents its own set of challenges, and given that the mission is currently in pre-Phase A, only a limited subset has been selected for preliminary analysis.

Also, at this stage, only the use of chemical propulsion is considered onboard. While electric propulsion could enable the design of low-thrust trajectories with potential for significant propellant savings, such an approach requires detailed inputs from the spacecraft system, which are not yet available at this early phase of the mission. For this reason, low-thrust transfer options have not been explored in the current analysis.

Furthermore, it is important to emphasise that the transfer design is highly sensitive to both the choice of launcher and the definition of the operational orbit. As these elements are still under definition, the analysis remains preliminary and will be refined as the mission architecture matures.

Considering the above, the following transfer options were investigated:

- **OPTION A:**
  - **Launch:** dedicated or rideshare launch to the WSB or TLI, for then reaching the operational orbit with a low-energy transfer. Ariane 6 is considered a possible option for a launcher, having an orbit with the following characteristics, defined in the ECI reference frame:
    - Apocenter altitude: 400000 km
    - Pericentre altitude: 200 km
    - Inclination: 6°
    - Both $\Omega$ and $\omega$ are set to zero, in search of a solution which is as general as possible. It is important to note that the relative geometry between the TLI orbit and the Moon evolves throughout the year, which in turn affects the transfer cost.
  - **Operational orbit:** the orbit considered is the one defined in Table 5, OPTION 1 for the operational orbit selection.
- **OPTION B:**
  - **Launcher:** rideshare launch to an LLO
  - **Operational orbit:** the operational orbit will depend on the insertion orbit provided by the launcher, which is still to be defined.
- **OPTION C:**
  - **Launcher:** dedicated launch to the preferred LLO
  - **Operational orbit:** in this case, the choice of the operational orbit is left entirely to the LunPAN mission. The orbit may be designed to resemble either that presented as OPTION 1 or that defined as OPTION 2, depending on which aspects are considered predominant.

For all options, the transfer injection date is assumed to fall between January 1, 2029, and January 1, 2030.

### 6.1 OPTION A

For OPTION A, two different types of transfer are considered: the direct transfer and a low-energy EM-$L_1$ invariant manifold transfer.

#### 6.1.1 Direct transfer

Direct transfer [19] is modelled as a sequence of manoeuvres resembling a classical Hohmann transfer. Although this method results in a high $\Delta V$ budget and is therefore suboptimal for a small spacecraft mission, it nevertheless provides a useful upper bound estimate of the $\Delta V$ requirements for an EM transfer.

The trajectory is designed within the EM rotating reference frame, and the spacecraft's motion is propagated in the CR3BP. The initial step involves propagating the launcher trajectory, initially known as a set of Keplerian elements, in the CR3BP framework. This implies a change of coordinates, followed by an iterative algorithm that adjusts the launch trajectory's initial conditions to produce a closed orbit under the CR3BP for at least one orbital period, while preserving the same apogee and perigee radii as those of the initially considered orbit. This transformation is necessary because the launcher orbit features an extremely high apocenter, which extends beyond the Moon's orbit, making the perturbative effects of the Moon non-negligible and requiring the use of a three-body dynamical model.

Table 8. EM transfers to LLOs - Summary

| **Type of transfer from Earth to an LLO** | | | **ToF [days]** | **LOI $\Delta V$ [m/s]** | **Missions which employed this transfer** |
|---|---|---|---|---|---|
| **Direct Hohmann-like transfer** | | | $\sim$2–6 [19] | $\sim$820+ [19] | Apollo missions |
| **Low-energy transfers** | **EM dynamics only is considered** | EM–$L_1/L_2$ invariant manifold transfer | TBD | TBD | - |
| | | Lunar capture, lunar fly-by | TBD | TBD | - |
| | **The SEM dynamics is considered** | WSB transfer, also known as BLT | >70–120 [19] | $\sim$640+ [19] | SMART-1, GRAIL, CAPSTONE etc. |
| **Direct insertion by the launcher** | Rideshare launch | | - | - | - |
| | Dedicated launch | | - | - | - |

Also, in the rotating reference frame, the $x$-axis is fixed along the EM line, meaning that the geometry of the departure orbit varies with the departure date due to the rotation of the ECI frame with respect to the rotating one. The following procedure has been defined to fix the TLI orbit in the CR3BP framework:

- The Keplerian elements of the launcher orbit are derived based on the information provided previously. These orbital elements are first converted into a Cartesian state vector in the ECI reference frame.
- This Cartesian state is then transformed into the EM rotating reference frame to enable propagation under the CR3BP dynamical model.
  The launcher trajectory is then numerically propagated within the CR3BP framework.
- An iterative procedure is employed to adjust the apogee and perigee radii of the launcher orbit, ensuring consistency with the given data. This correction step is introduced to minimise the effect of the non-Keplerian dynamical model on the launcher orbit.

Once the launcher orbit is defined in the EM rotating reference frame, the transfer is designed as a Hohmann-like transfer: a first impulse, $\Delta V_{TLI}$, is given at the pericenter of the launcher orbit, i.e. at TLI, to insert the spacecraft into a direct transfer to the Moon; a second impulse, $\Delta V_{LOI}$, is given once the LLO of interest is reached, to insert the spacecraft into it. Initial guesses for $\Delta V$ are found thanks to the two-body problem approximation, picturing a transfer subject to Keplerian dynamics. Such initial guesses are then refined through an optimisation process involving the CR3BP dynamics. Figure 20 illustrates the evolution of the total $\Delta V$ needed for the transfer, sum of $\Delta V_{TLI}$ and $\Delta V_{LOI}$, as a function of the date at which the spacecraft is inserted by the launcher in the transfer trajectory, i.e. the transfer injection date.

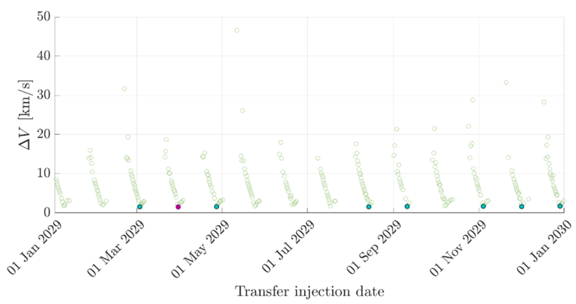


Fig. 20. Evolution of the direct transfer cost as a function of the transfer injection date.

All green dots in Figure 20 represent the possible transfer options. The pink dot identifies the solution with the lowest total $\Delta V$, while the blue dots are the seven conditions, following the best one, characterised by the lowest total $\Delta V$. The evolution of the transfer cost exhibits a periodic pattern matching the Moon's revolution period around the Earth, equal to 27.32 days. This result was expected for the direct transfer and, in a way, serves as a validation of the analysis conducted.
However, certain minima in the cost evolution appear to be more favourable than others. This can be attributed to variations in the inclination of the initial orbit with respect to the EM plane, corresponding to the $xy$ plane in the rotating reference frame, over the year.
Nevertheless, further analysis is needed to confirm these findings. Data about the lowest-$\Delta V$ direct transfer are reported in Table 9. The same is then shown in Figure 21.

Note that, in this case, $\Delta V_{TLI} = 0.043$, km/s and

Table 9. Lowest $\Delta V$ direct transfer - Total $\Delta V$ required, transfer time and transfer injection date.

| Transfer injection date [UTC] | Transfer ToF | $\Delta V_{TOT}$ [km/s] |
|---|---|---|
| 30-Mar-2029 12h | 2 days 4 hours | 1.57 |

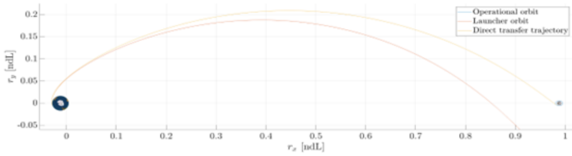


Fig. 21. Direct transfer - Lowest ΔV option.

$\Delta V_{LOI} = 1.48$km/s. Even assuming that the TLI impulse is entirely provided by the launcher, the LOI manoeuvrer alone requires a $\Delta V$ that exceeds the capabilities of the propulsion system typically available on a mini-satellite. This value can therefore be regarded as an upper admissible limit for $\Delta V_{LOI}$: strategies with a higher $\Delta V$ will be considered suboptimal.

### 6.1.2 Low-energy EM-$L_1$ invariant manifold transfer

The low-energy EM-$L_1$ invariant manifold transfer concept investigated in this Section is based on the idea of connecting the launcher orbit with the stable manifold of a Halo orbit around EM-$L_1$. A second leg of the transfer trajectory will follow, where the unstable manifold of the same Halo orbit is linked to the selected operational LLO. The launcher orbit is first defined and refined within the CR3BP framework, as outlined in the previous section.

Once the departure orbit is defined, the family of Halo orbits around EM-$L_1$ is analysed. Halo orbits that are either inherently stable, i.e. with a stability index lower than one [20], are excluded. At the same time, while instability is a necessary feature, since it enables the use of the orbit's manifolds to design a transfer trajectory, orbits characterised by excessive chaoticity yield results which are difficult to predict and reproduce, making them unsuitable for reliable trajectory design.

To identify the most suitable Halo orbit, the minimum distance to the Moon is computed for each candidate orbit. The Halo orbit whose minimum lunar distance most closely matches that of the target LLO is selected as the baseline for transfer trajectory design.

The direction of the stable manifold is determined by evaluating the eigenvector corresponding to the smaller real eigenvalue of the monodromy matrix associated with the selected Halo orbit. A total of 361 points are sampled uniformly along the Halo orbit and slightly perturbed in the direction of the stable eigenvector. These perturbed states are then propagated backwards in time for 90 days, producing a set of stable manifold trajectories.

For each stable manifold trajectory, the distance between each of its points and every point along the launcher orbit is computed. The goal is to identify, for each manifold trajectory, the condition that minimises the spatial separation from the launcher orbit. States for which the $\Delta V$ required to bridge the gap between the launcher orbit and the stable manifold is more than 2 km/s are discarded. Once such a condition is identified, it is used as an initial guess for a numerical optimisation aimed at minimising the required $\Delta V$ to connect the two trajectory branches.

This analysis is repeated across 730 potential launch dates, assuming injection into the stable trajectory can be located everywhere on the launcher trajectory. The evolution of the required $\Delta V$ as a function of the transfer injection date is presented in Figure 22.

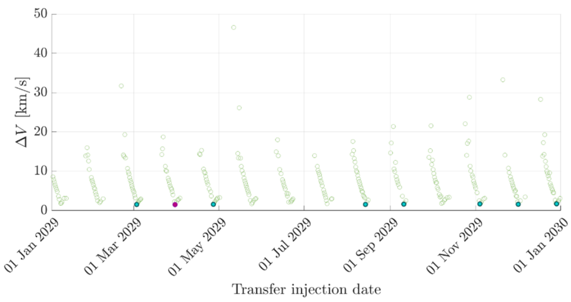


Fig. 22. Evolution of the low-energy transfer $\Delta V_1$ as a function of the transfer injection date.

The $\Delta V$ values shown correspond to the manoeuvre needed to insert the spacecraft from the launcher orbit into the stable manifold trajectory. As for the direct transfer, the pink dot represents the most efficient transfer in terms of $\Delta V$, while the five next-best options are highlighted as blue dots.

In this case, due to the nature of the transfer, it is more challenging to show a clear relationship between the cost and the EM orbital period. At this stage, the spacecraft has reached the selected Halo orbit around $L_1$. A second impulse is applied at the pericenter of this orbit, in the direction of the forward-propagated unstable manifold. The magnitude of this second impulse is determined by calculating the $\Delta V$ required to insert the spacecraft into an orbit with a mean distance from the Moon similar to that of the LLO defined in Table 5.

However, the plane change manoeuvre necessary to transition from the inclination naturally reached by the trajectory considered to the one defined in Table 5 proves to be excessively expensive in terms of $\Delta V$. Consequently, it is decided not to perform the plane change. In this way, the trajectory is designed to reach an orbit where the spacecraft's distance from the Moon meets the payload requirements, while the variability in the evolution of orbital parameters due to perturbations still needs to be verified. The Keplerian parameters characterising the orbit reached are defined in Section 6.1.2.

Table 10. Orbital parameters of the orbit reached by the low-energy transfer.

| $a$ [km] | $e$ [-] | $i$[°] | $\Omega$[°] | $\omega$[°] |
|---|---|---|---|---|
| 2577.5 | 0.0314 | 95.19 | 89.03 | 276.11 |

Finally, some parameters characterising the low-energy transfer are reported in Section 6.1.2. Figure 23 shows the overall transfer.

Table 11. Lowest $\Delta V$ low-energy transfer - Total $\Delta V$ required, transfer time and transfer injection date.

| Transfer injection date [UTC] | Transfer ToF | $\Delta V_{TOT}$ [km/s] |
|---|---|---|
| 2029-Sept-12 12h | 87 days 1.5 hour | 1.721 |

Table 12. $\Delta V$ to be given at different stages of the transfer.

| Impulse | $\Delta V$ [km/s] | Description |
|---|---|---|
| $\Delta V_{TLI}$ | 1.16 | To insert the spacecraft from the launcher orbit to the EM-$L_1$ Halo stable manifold |
| $\Delta V_{LOI}$ | 0.558 | To insert the spacecraft from the EM-$L_1$ Halo unstable manifold to a high polar LLO |

Table 13. Transfer times along the various trajectory phases.

| Phase | Duration | Description |
|---|---|---|
| $t_1$ | 4 days 17.8 hours | Time spent on the launcher orbit |
| $t_2$ | 74 days 8.8 hours | Time spent on the EM-$L_1$ Halo stable manifold |
| $t_3$ | 7 days 23.1 hours | Time spent on the EM-$L_1$ Halo unstable manifold |

It is important to highlight that both the total $\Delta V$ required for the transfer and its duration are not compatible with a small satellite mission, such as the one analysed in this study, even when considering only $\Delta V_{LOI}$. Unfortunately, in this specific case, the use of the described technique proves less advantageous than initially expected. Nevertheless, it provides a secondary upper bound for the $\Delta V_{LOI}$, lower when compared to that of the direct transfer.
Nevertheless, alternative techniques can be employed to identify lower-cost transfer trajectories. Possible options include a WSB transfer, a trajectory incorporating multiple lunar flybys, or a free-return trajectory, among others. To obtain a comprehensive understanding of the factors defining the mission cost, a far more extensive set of analyses would be required beyond those described herein. It is proposed to conduct such analyses as part of future work.

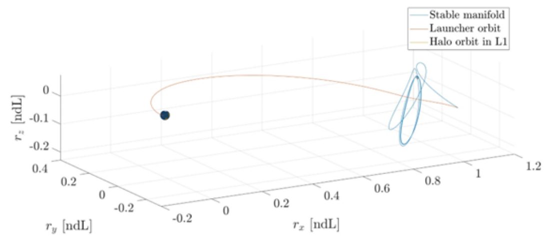


Fig. 23. Low-energy transfer - Lowest ΔV option.

### *6.2 OPTION B*

OPTION B considers a scenario in which a rideshare or a dedicated launch would directly insert LunPAN into an LLO.
In the rideshare case, the spacecraft would be deployed into an LLO defined by the requirements of a primary mission, whose characteristics are still to be fully determined. Possible operational orbits were previously reported as CASE 1 and CASE 2 under OPTION 2 for the operational orbit selection. It is also possible, assuming the launcher does not leave the spacecraft in a configuration that remains bounded in the long term, to consider modifying the orbit's shape to achieve a quasi-frozen orbit. For a preliminary estimation of the $\Delta V$ budget required to change the orbit shape from that fixed by the primary mission to one which is more convenient for LunPAN purposes, it is assumed that the launcher injects the spacecraft into a circular orbit at 100 km altitude, with an inclination of 36° in the MoonMJ2000Eq reference frame. Since the target LLO inclination is already fixed, and a change in inclination is expensive from the $\Delta V$ budget point of view, the focus of this analysis is on modifying the orbital shape while keeping the inclination constrained. In this scenario, no proper "transfer" is required; instead, a shape-change manoeuvre is performed to raise the apogee of the injection orbit to that of the operational orbit, thereby achieving the desired orbital geometry and ensuring long-term stability. As for the inclination, the right ascension of the ascending node is also assumed to be fixed to match that of the final operational orbit. If this is not possible, the costs required to move the spacecraft from the launcher insertion orbit to the operational one will be greater than what will be defined in this Section. The target is first to design an operational orbit that remains bounded for the overall mission duration, i.e. three years, with the ob-

jective of reducing and ideally avoiding station-keeping costs. This can be achieved by targeting an elliptical orbit, so that the role of the lunar gravitational harmonics is not dominant, and setting properly the orientation of the spacecraft, that is, the longitude of the ascending node and the argument of pericenter.

The pericenter altitude is assumed to remain equal to that of the initial LLO in which the launcher inserts the spacecraft. Consequently, a manoeuvre at pericenter, tangent to the velocity direction, will be required to increase the orbit's apocenter radius. The manoeuvre entity is a function of the target apocenter altitude, as shown in Table 14.

Table 14. Apocenter raise manoeuvre $\Delta V$.

| **Id** | **Final apocenter altitude [km]** | $\Delta V$ **[km/s]** |
|---|---|---|
| **1** | 300 | 0.042 |
| **2** | 500 | 0.078 |
| **3** | 800 | 0.126 |

The manoeuvrer is preliminarily computed as a simple one-impulse transfer, considering only two-body dynamics. Preliminary simulations performed with GMAT, using the full model described in Section 5.1.2, showed that zero station-keeping costs can be achieved, for example, with $\Omega = 0°$ and $\omega = 240°$, or $\Omega = 0°$ and $\omega = 310°$.
Achieving these conditions is possible since the initial orbit provided by the launcher is assumed circular, because a circular orbit does not have a predefined argument of pericenter. The desired value of the argument of pericenter could then be chosen depending on when the manoeuvrer is applied along the orbit, for example, when the spacecraft is at a southern latitude. However, from a communications standpoint, it is preferable to have the apocenter oriented toward the southern hemisphere. Based on the current investigations, having this orientation does not correspond to a stable orbit, which implies that a dedicated budget for station-keeping would be required. A very preliminary strategy is used to establish a $\Delta V$ budget for station-keeping, providing a first estimate of the associated cost. To do so, it is assumed that once a year, the pericenter of the operational orbit reaches a low altitude of approximately 40 km. The station-keeping costs are assumed to correspond to the cost of the manoeuvre required to raise the pericenter of the orbit to an altitude of 100 km and to adjust its apocenter, which is also found to be slightly variated. Let's consider that, identified by the same Id as in Table 14, within one year, the operational orbits are modified by the perturbation effects such that their semimajor axis and eccentricity are such in Table 15.

Table 15. Hypothetical orbit parameters after 1 year.

| **Id** | $a$ **[km]** | $e$ **[-]** |
|---|---|---|
| **1** | 1938 | 0.085 |
| **2** | 2037 | 0.13 |
| **3** | 2188 | 0.19 |

The cost of the hypothetical station-keeping manoeuvre required to return the spacecraft to the corrected operational orbit is computed as a simple two-impulse Hohmann transfer, having the $\Delta V$ costs reported in Table 16.

Table 16. Station-keeping $\Delta V$ – 1 year.

| **Id** | $\Delta V$ **needed for one hypothetical station-keeping manoeuvre [km/s]** |
|---|---|
| **1** | 0.0265 |
| **2** | 0.0248 |
| **3** | 0.0227 |

Given the total duration of the mission, the hypothetical station-keeping costs are to be multiplied by three. This factor depends on the semi-major axis and initial orientation, which is yet to be defined, because the eccentricity can reach the values displayed in Table 15 faster depending on the initial condition, as shown in Figure 24.
A contingency analysis, accounting for uncertainties in position and velocity due to orbit determination and manoeuvrer execution, along with a more detailed station-keeping assessment, will be conducted at a later stage of the mission for the orbits presented in this Section.

## 7. Post-mission disposal

For LLO, the easiest strategy to implement for disposal at end-of-life is a lunar impact, paying attention to preserve the historical sites.
In Figure 25, a preliminary estimate of the $\Delta V$ needed to impact on the Moon is shown, as a function of the initial altitude. Similarly to what has been studied for high-altitude orbits in the Earth neighbourhood [21], it is possible to reduce the de-orbiting cost by wisely exploiting the third-body effect.

In all options considered for the operational orbit, since frozen conditions are preferred to reduce station-keeping costs, the mission shall be envisaged in such a way that, once the 3 years mission lifespan is concluded, the orbit is moved towards a more beneficial condition for the end of life, in terms of eccentricity and inclination. Note that the preliminary simulations performed show that the inclination changes naturally during the lifetime of the satellite, at least for some initial conditions. If needed, this change can be leveraged to reduce disposal costs.

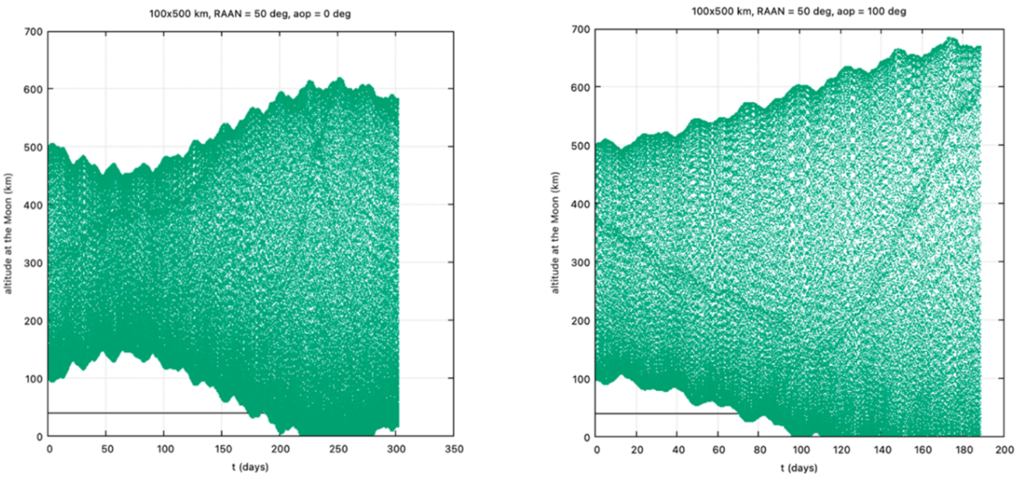


Fig. 24. Altitude at the Moon evolution, for two different initial orbit orientations.

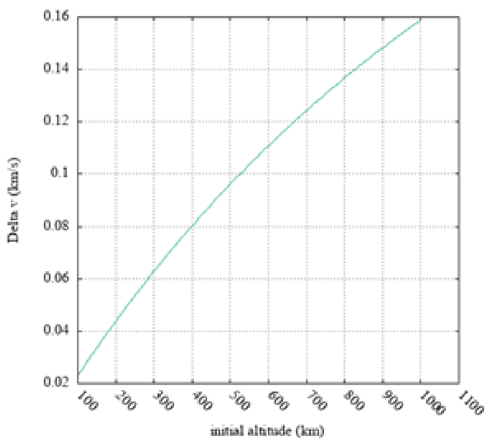


Fig. 25. Disposal $\Delta V$ as a function of the operational orbit initial altitude

Finally, if the altitude is low enough, it is possible to design a "natural" de-orbiting towards the Moon, whose duration will depend on the specific orientation of the orbit.

## 8. Final trade-off

In conclusion to the discussions presented in the previous sections, a final trade-off is provided to summarise the main outcomes in Tables 17 to 19. When related to ✓, a certain option is considered good; $\sim$ is related to achievable but sub-optimal solutions and $\times$ with not achievable options.

Table 17 reports the final trade-off related to the selection of the operational orbit, taking into account the considerations on particle flux, station-keeping requirements, and disposal strategies. LLOs are the most suitable option when considering the scientific objectives related to particle flux measurements. However, their adoption comes at the cost of increased operational challenges, particularly in terms of station-keeping and overall mission design complexity. Anyway, the scientific return of LLOs makes them the preferred choice as operational orbits compared to NRHOs.

In Table 18, a final trade-off on transfer strategies is presented, assuming an LLO as the operational orbit. Considering additional requirements from system design and launcher availability, a rideshare or dedicated launch transfer is preferred over an autonomous one. However, this choice limits the possibility of selecting the option that would otherwise appear most advantageous from the perspective of the operational orbit. In the next mission phases, further effort will be devoted to refining this aspect.

Finally, Table 18 also includes information on transfer options to NRHOs, allowing a complete assessment of the advantages and drawbacks of the operational orbit choice from the perspective of the transfer strategy selection as well.

## 9. Conclusions and future works

This paper has presented a set of techniques for the design of a scientific mission whose primary requirement is to maintain, throughout its duration, a very low mean altitude with respect to the Moon. This requirement naturally leads to the selection of a LLO as the operational orbit. A procedure has been discussed to identify, in a straightforward way, nominal frozen-like conditions that remain bounded over the long term, despite the strong perturbations affecting LLOs, generated both from third-body effects and from the lunar gravity field, while ensuring that the required station-keeping effort remains limited.

The choice of the operational orbit has been made

Table 17. Operational orbit selection, final trade-off.

| Operational orbit | | Flux | Station-keeping | Disposal |
|---|---|---|---|---|
| **High altitude frozen LLO (1000 km)** | | ✓ | ✓ → If a frozen condition can be achieved, the cost for maintaining the orbit would theoretically be zero | $\sim \rightarrow$ Lunar impact, 150 m/s. |
| **Eccentric low altitude LLO (100 km)** | Quasi-frozen condition | ✓ | $\sim \rightarrow$ A frozen condition seems very promising, but must be consolidated with further simulations. If a frozen condition is not achieved, the estimated station-keeping cost is about 150 m/s per year [13]. | ✓ → Lunar impact, 20 m/s, it is important to avoid impacting on historical sites. |
| | Not frozen condition (i.e. apocenter in the southern hemisphere) | ✓ | $\sim \rightarrow$ station-keeping cost could range between 150 m/s [13] to 250 m/s per year. | ✓ → Lunar impact, since the spacecraft is not in frozen conditions, disposal could even be cost-free. |
| **NRHO** | | $\sim$ | ✓ → $\sim 1-3$ m/s per year [22, 23] | ✓ → Lunar impact, 15 m/s [24] |

Table 18. Transfer selection to LLO, final trade-off.

| **Transfer type** | **Coasting time** | **$\Delta V$ to be provided by the on-board thrusters** |
|---|---|---|
| Direct Hohmann-like transfer | ✓ → $\sim 2-3$ days | $\times \rightarrow \sim 1.5$ km/s |
| Low energy transfer | $\times \rightarrow \sim 80-120$ days | $\times \rightarrow \sim 0.65-1$ km/s |
| Rideshare launch | ✓ → Time needed to adjust the orbit shape: $\sim 1-2$ days | ✓ → To adjust the orbit shape: 100 m/s |
| Dedicated launch | ✓ → There is no coasting time | ✓ → There is no $\Delta V$ to be provided before the beginning of operations |

by carefully balancing both scientific and system-level requirements. Furthermore, different strategies for the transfer from Earth to a LLO have been investigated. Several options were analysed and compared, either through dedicated numerical simulations and optimisation or by relying on existing literature.

Finally, a conclusive trade-off has allowed the identification of the transfer strategy that best fits the mission objectives, while still being suboptimal from some points of view. In the next phases of the mission, the design of the operational orbit will be further refined to completely evaluate and minimise the station-keeping costs. Also, additional transfer strategies will be carefully assessed thanks to numerical simulations, provided they are considered feasible from a system perspective.

## 10. Acknowledgements

This research has received funding as part of a study funded by the European Space Agency within a new initiative on Small Missions for Exploration, and its inception, Destination the Moon. The authors would also like to thank all the other members of the team who contributed to the pre-Phase A design of the LunPAN spacecraft. In particular, we are grateful to the colleagues from the University of Geneva (UNIGE) for their support in computing the particle flux as a function of the orbital mean distance from the Moon and, together with colleagues from the Czech Technical University in Prague (CVUT), were responsible for the design of the spacecraft payload, and to Aerospacelab for their valuable contribution to the assessment of launcher options and the design of the spacecraft systems.

Table 19. Transfer selection to NRHO, final trade-off.

| **Transfer type** | **Coasting time** | **$\Delta V$ to be provided by the on-board thrusters** |
|---|---|---|
| Low-energy transfer - EM manifolds dynamics | $\sim \to \sim$ 120 days | $\times \to \sim$ 0.83 km/s [25] |
| WSB transfer | $\sim \to \sim 80 - 120$ days | ✓$\to \sim$ 0.04 km/s |

## References


[1] "Artemis mission - NASA," https://www.nasa.gov/humans-in-space/artemis/. Last accessed: 21 August 2025.

[2] "Gateway - NASA," https://www.nasa.gov/mission/gateway/. Last accessed: 21 August 2025.

[3] Hulsman, J., Wu, X., Azzarello, P., Bergmann, B., Campbell, M., Clark, G., Cadoux, F., Ilzawa, T., Kollmann, P., Llopart, X., Nénon, Q., Paniccia, M., Roussos, E., Smolyanskiy, P., Sukhonos, D., and Thonet, P. A., "Relativistic particle measurement in Jupiter's magnetosphere with Pix.PAN," *Experimental Astronomy*, Vol. 56, No. 2, 2023, pp. 371–402, doi: https://doi.org/10.1007/s10686-023-09918-4.

[4] Folta, D. and Quinn, D., "Lunar Frozen Orbits," *AIAA/AAS Astrodynamics Specialist Conference and Exhibit, Keystone, Colorado*, 2006, doi: https://arc.aiaa.org/doi/abs/10.2514/6.2006-6749.

[5] Lidov, M., "The evolution of orbits of artificial satellites of planets under the action of gravitational perturbations of external bodies," *Planetary and Space Science*, Vol. 9, No. 10, 1962, pp. 719–759, doi: https://doi.org/10.1016/0032-0633(62)90129-0.

[6] Roth, E. A., "Launch window study for the highly eccentric orbit satellite HEOS-1," *Celestial mechanics*, Vol. 2, No. 3, 1970, pp. 369–381, doi: https://doi.org/10.1007/BF01235137.

[7] Janin, G., "The stability of eccentric polar orbits around the Moon," *Acta Astronautica*, Vol. 9, No. 6, 1982, pp. 421–423, doi: https://doi.org/10.1016/0094-5765(82)90071-6.

[8] De Almeida Prado, A. F. B., "Third-Body Perturbation in Orbits Around Natural Satellites," *Journal of Guidance, Control, and Dynamics*, Vol. 26, No. 1, 2003, pp. 33–40, doi: https://doi.org/10.2514/2.5042.

[9] https://software.nasa.gov/software/GSC-19097-1. Last accessed: 20 August 2025.

[10] Konopliv, A., Asmar, S., Carranza, E., Sjogren, W., and Yuan, D., "Recent Gravity Models as a Result of the Lunar Prospector Mission," *Icarus*, Vol. 150, No. 1, 2001, pp. 1–18, doi: https://doi.org/10.1006/icar.2000.6573.

[11] Pergola, P. and Alessi, E., "Libration point orbit characterization in the Earth-Moon system," *Monthly Notices of the Royal Astronomical Society*, Vol. 426, No. 2, 2012, pp. 1212–1222, doi: https://doi.org/10.1111/j.1365-2966.2012.21585.x.

[12] Vallado, D. A., *Fundamentals of Astrodynamics and Applications (4th ed.)*, Space Technology Library, 2013.

[13] Beckman, M., "Stationkeeping for the Lunar Reconnaissance Orbiter (LRO)," *20th International Symposium on Space Flight Dynamics, Annapolis, Maryland*, 2007.

[14] Dono, A., "Lunar Orbit Stability for Small Satellite Mission Design," *Interplanetary CubeSat Workshop-iCubeSat, Imperial College of London, United Kingdom*, 2015.

[15] Lara, M., De Saedeleer, B., and Ferrer, S., "Preliminary design of low lunar orbits," *21st International Symposium on Space Flight Dynamics*, 2009.

[16] Belbruno, E., Gidea, M., and Topputo, F., "Weak Stability Boundary and Invariant Manifolds," *SIAM Journal on Applied Dynamical Systems*, Vol. 9, No. 3, 2010, pp. 1061–1089, doi: https://doi.org/10.1137/090780638.

[17] Conley, C. C., "Low Energy Transit Orbits in the Restricted Three-Body Problems," *SIAM Journal on Applied Mathematics*, Vol. 16, No. 4, 1968, pp. 732–746, doi: https://doi.org/10.1137/0116060.

[18] Fantino, E., Gómez, G., Masdemont, J., and Ren, Y., "A note on libration point orbits, temporary capture and low-energy transfers," *Acta Astronautica*, Vol. 67, No. 9, 2010, pp. 1038–1052, doi: https://doi.org/10.1016/j.actaastro.2010.06.037.

[19] Parker, J. S. and Rodney, L. A., *Low-energy lunar trajectory design*, John Wiley  Sons, 2014.

[20] Connor Howell, K., "Three-dimensional, periodic,'halo'orbits," *Celestial mechanics*, Vol. 32, No. 1, 1984, pp. 53–71, doi: https://doi.org/10.1007/BF01358403.

[21] Alessi, E. M., Deleflie, F., Rosengren, A. J., Rossi, A., Valsecchi, G. B., Daquin, J., and Merz, K., "A numerical investigation on the eccentricity growth of GNSS disposal orbits," *Celestial Mechanics and Dynamical Astronomy*, Vol. 125, No. 1, 2016, pp. 71–90, doi: https://doi.org/10.1007/s10569-016-9673-4.

[22] Bucci, L., Lavagna, M., and Jehn, R., "Station keeping techniques for Near Rectilinear Orbits in the Earth-Moon system," *10th International ESA Conference on Guidance, Navigation and Control Systems, Salzburg, Austria*, 2017.

[23] Newman, C., Davis, D. C., Whitley, R., Guinn, J., and Ryne, M. S., "Stationkeeping, orbit determination, and attitude control for spacecraft in Near Rectilinear Halo Orbits," *AAS Astrodynamics Specialists Conference, Snowbird, Utah*, 2018.

[24] Boudad, K. K., Davis, D. C., and Howell, K. C., "Disposal Trajectories from Near Rectilinear Halo Orbits," *AAS/AIAA Astrodynamics Specialists Conference, Snowbird, Utah*, 2018.

[25] Arikan, E., *Transfer trajectory and operational orbit selection for Earth-Moon L2 near rectilinear halo orbits through invariant manifolds*, Master's thesis, Politecnico di Milano, Space Engineering, 2023, Supervisor: C. Colombo, Co-advisor: E. M. Alessi. Available at: https://www.politesi.polimi.it/handle/10589/208238.